LYCEN/9412
Avril 1994

Correlation between phase transformation and stress evolution in nitrogen implanted iron.

J. Jagielski

Institute for Electronic Materials Technology, Wolczynska 133, 01-919 Warsaw, Poland

S. Fayeulle

Département Matériaux-Mécanique-Physique, Ecole Centrale de Lyon, UA CNRS 447, B.P. 163, 69131 Ecully Cedex, France

G. Marest, N. Moncoffre

Institut de Physique Nucléaire IN2P3-CNRS et Université Claude Bernard Lyon-1
43 Bd du 11 Novembre 1918, 69622 Villeurbanne Cedex, France

FERMILAB
LIBRARY
JUN 28 1994

Abstract

Phase transformations and iron lattice parameters for nitrogen implanted XC06 steel were simultaneously studied by means of CEMS and GIXD techniques. The results revealed that the transformation from ε-$Fe_{3-x}N$ into ε- or ζ-Fe_2N phase correlates with stress relaxation. Such an observation indicates that this transformation is induced by a compressive stress created by the N ions implanted into Fe matrix. Mechanism and possible practical implications of this effect are discussed.

Submitted to Materials Science and Engineering A

I. INTRODUCTION

Nitrogen implantation into iron base alloys has been recognized for several years as an attractive new technology which allows to improve significantly the mechanical properties of metals. The numerous applications demonstrate that the improvement of metal properties obtained after implantation is repeatable and economically interesting, especially in the field of wear reduction [1-3]. The practical applications, however, have forwarded the full understanding of physical processes occurring during implantation and numerous interesting questions are still open. One of them is the problem of phase transformation in the Fe-N system. Recently a "phase diagram" of nitrogen implanted iron has been proposed [4] showing a rather abrupt transformation from magnetic ε-$Fe_{3-x}N$ phase into a paramagnetic ε- or ζ-Fe_2N phase. It should be noted that these phases are markedly different; in addition to their magnetic properties their structural parameters are distinct [5,6]. Thus the reasons of such a transformation seem to be a more complex phenomenon than a simple increase of the nitrogen concentration. The aim of this paper is to present a specific study of the $Fe_{3-x}N$ to Fe_2N phase transformation.

II. EXPERIMENTAL

XC06 steel samples (AISI 1006 : 0.05% C, 0.205% Si. 0.375% Mn, 0.045% Ni and 0.07% Cr) were used. Prior to implantation samples were annealed at 600°C during 1 hour in hydrogen atmosphere then polish with diamond paste. Samples were implanted at room temperature with 50 keV $^{15}N^+$ ions (R_p = 57 nm, ΔR_p = 25 nm) by using the isotope separator of the Institut de Physique Nucléaire de Lyon to doses ranging from 0.5×10^{17} at./cm^2 up to 4×10^{17} at/cm^2. Care was taken to avoid an excessive heating during the implantation process.

The Conversion Electron Mössbauer Spectroscopy (CEMS) technique was used to determine the phase transformations in implanted samples. The CEMS measurements were performed at room temperature (RT) by using a gas flow electron counter with He-6%CH_4

gas. A conventional constant acceleration Mössbauer spectrometer was used. All isomer shift data are given with respect to the α-Fe standard.

The samples were also analyzed by means of Grazing Incidence X-ray Diffraction (GIXD) method. The measurements were performed with grazing angle diffractometer using Cu K X-ray radiation (=0.15406 nm). The diffraction spectra were recorded at two different incident angles: 0.5^{o} and 2° which correspond to the penetration depths of 50 nm and 200 nm respectively.

III. RESULTS

The CEMS spectra recorded for the implanted samples are shown in Fig. 1. The spectra were fitted with the use of the parameters previously reported in the literature. The set of these parameters can be found in references. 4 and 7. At low implantation doses ($5x10^{16}$ at/cm^2-$1x10^{17}$ at./cm^2) (Fig. 1b,c) the spectra were deconvoluted into three magnetic components: two corresponding to the host matrix and one due to the α'-martensite/α''-$Fe_{16}N_2$ phases. At $2x10^{17}$ at./cm^2 (Fig. 1d) the ε-$Fe_{3-x}N$ phase appeared at the expense of martensite/$Fe_{16}N_2$ phases. A drastic change occured at $3x10^{17}$ at./cm^2 (Fig 1e) when ε- or ζ-Fe_2N phase was detected, contributing to about 27% to the total spectral area. The Fe_2N phase was formed at the expense of ε-$Fe_{3-x}N$ which contribution decreased from 52% to 38%. Increasing the implantation dose up to $4x10^{17}$ at./cm^2 (Fig. 1f) resulted in the further transformation of ε-$Fe_{3-x}N$ into Fe_2N which became the dominant nitride phase, contributing to 47% to the spectral area. Relative contributions of the different phases are presented in Fig. 2.

The next part of the experiment was devoted to the study of the lattice parameters of the implanted structure by means of GIXD. Previous works [8-10] report on results obtained on the same Fe-N system by such a technique. X-ray diffraction spectra obtained for the various samples are presented in Fig. 3. It can be noted that the nitride phases (especially ε-$Fe_{3-x}N$) formed during implantation have interreticular spacings very close to those

characteristic of pure iron. The diffraction spectra obtained for low and medium doses are composed of large diffraction peaks corresponding to an overlapping of numerous lines in the vicinity of that characteristic of α-Fe (Fig. 3a). At $4x10^{17}$ N^+/cm^2 when Fe_2N becomes the dominant nitride phase, the diffraction peaks are narrower, and those obtained for nitride phase are well separated from that of α-Fe.

It should be noted that CEMS and GIXD measurements do not allow to determine whether the Fe_2N phase formed is of the ε or of the ζ type. CEMS parameters of both phases are similar whereas GIXD experimental results show better agreement with ζ-Fe_2N data than with those of ε-Fe_2N. In order to study the strain induced by the implantation process the lattice parameters should be determined with the precision of 0.0001 nm. The large peaks obtained for the implanted layer only (incidence angle equal to 0.5°) makes such a determination impossible. Therefore the lattice parameter of the iron lattice (d_{Fe}) was calculated from spectra measured at the incidence angle of 2° (i.e. corresponding to the iron layer below the implanted zone) (fig.3b). If stress exits in the implanted layer, it is balanced by opposite stress in the underlaying layers. Hence measurements performed at 2° will give the strain ($\varepsilon=(d_{Fe}-d_0)/d_0$, with d_0 the lattice parameter of the non implanted sample) just below the implanted zone which can be used to monitor the stress in the upper part of the sample. The value of d_{Fe} was determined by fitting the diffraction peak with a Gaussian function. Thick lines on Fig. 4 present the results of the fits. The fit region was slightly displaced towards the higher angles to diminish the influence of the peaks due to the ε-$Fe_{3-x}N$ phase (fig.3) The evolution of versus implantation dose is shown in Fig. 5. The positive value of ε demonstrates that compressive stresses exit in the implanted layer. Four distinct regions can be noticed: the rapid increase of ε from 0 up to $1.45x10^{-3}$ for the first implanted dose of $5x10^{16}$ at./cm^2, a region of slow increase up to $1.7x10^{-3}$ for doses varying from $5x10^{16}$ at./cm^2 to $2x10^{17}$ at./cm^2, followed by the decrease to $1.02x10^{-3}$ at $3x10^{17}$ at./cm^2 and further reincrease at the highest implantation dose of $4x10^{17}$ at./cm^2. Such a behavior reflects the evolution of stress induced by implantation in the outermost layer of the sample: increase when the implantation dose varies from 0 to $2x10^{17}$ at./cm^2, partial stress relaxation at $3x10^{17}$ at./cm^2 , new increase at $4x10^{17}$ at./cm^2.

IV. DISCUSSION

The comparison of the strain evolution (Fig. 5) with the phase abundance (Fig. 2) leads to the conclusion that the stress relaxation correlates with the beginning of the transformation from $Fe_{3-x}N$ to Fe_2N. It is thus very likely that this transformation is induced by the stress created by the incorporation of foreign nitrogen atoms into the iron lattice (for comparison see the results reported on stress induced amorphization by Linker [11]). In view of the results presented above we propose the following mechanism of the phase transformations occurring in nitrogen implanted iron. For low implantation doses the insertion of nitrogen atoms into iron matrix leads to the formation of martensitic and/or $Fe_{16}N_2$ phases and the iron host lattice becomes compressed. The noticeable stress observed in this stage can be explained by the fact that the phases keep very similar structure to that of pure iron (very small atomic displacements are required for transformation from α-Fe to α'/α'' martensitic/$Fe_{16}N_2$ phases), but with more and more nitrogen atoms placed in the iron cell. For doses ranging from $1x10^{17}$ at./cm^2 to $2x10^{17}$ at./cm^2 more distinct precipitates of ε-$Fe_{3-x}N$ are formed. Their structure is still close to that of the host iron matrix. The incorporation of an increasing number of nitrogen atoms thus results in the continuous accumulation of stress. Above $2x10^{17}$ at./cm^2 the stress becomes too high to maintain the structural order defined by cubic -Fe structure and the rearrangement of the nitride precipitates from ε-$Fe_{3-x}N$ to nitrogen richest ε-or ζ-Fe_2N nitride (fig.2) occurs leading to the partial stress relaxation. Very likely the stress relaxation is due to the fact that the part of nitrogen atoms which was in solution when the dominant phase was ε-$Fe_{3-x}N$ is now incorporated in the ε- or ζ-Fe_2N nitride precipitates. This interpretation is supported by two observations: i) a rapid increase of strain observed for low doses which suggests that an important contribution to strain comes from the nitrogen solution and ii) the ε- or ζ-Fe_2N phase contains more nitrogen atoms than the ε-$Fe_{3-x}N$ one, therefore such a transformation should be associated with a decrease of nitrogen concentration in the vicinity of the precipitates. For the highest implantation dose ($4x10^{17}$ at./cm^2) an almost complete transformation of the outermost layer ($\approx$ 40 nm) to ε- or ζ-Fe_2N nitride has occured as displayed by the GIXD spectrum (the α-Fe contribution is not detected at 0.5°,

fig.3a). In consequence incoming nitrogen atoms can only be located below the Fe_2N layer in martensite or in ε-$Fe_{3-x}N$ phases. The CEMS spectra show that the contributions of α-Fe and ε-$Fe_{3-x}N$ phases are still present at this highest dose. However they are probably located deeper in the sample since in the CEMS technique about 90% of conversion electrons are collected from roughly the 150 nm thick layer [12]. The increase of nitrogen content in the ε-$Fe_{3-x}N$ underlayer could explain the stress increase at $4x10^{17}$ at./cm^2 as detected by GIXD at 2°.

V. CONCLUSION

The major result of this paper is that the ε-$Fe_{3-x}N$ to Fe_2N phase transformation correlates with the stress relaxation. The formation of Fe_2N at the expense of ε-$Fe_{3-x}N$ may be thus defined as a stress induced process. Taking into account that stress level in surface layers is directly correlated with fatigue properties of materials our results could explain why an optimum implantation dose was observed [13] in fatigue experiments performed on nitrogen implanted steel. The evolution of strain displayed in Fig 5, proves that relatively low nitrogen doses are required for a significant increase of stress in the surface layer. Hence the improvement of fatigue properties should occur at rather low nitrogen doses. Most of wear experiments show that for high implantation doses the wear resistance reaches a constant level and does not decrease as for fatigue experiments. Apparently the wear resistance is much less sensitive on the stress level and more on the nitrogen concentration i.e on the nature of the precipitated phases.

ACKNOWLEDGEMENT

The authors wish to thank A. Plantier from IPN- Lyon for ion implantations

REFERENCES

1. J.K. Hirvonen, "Treatise on Material Science and Technology" Vol. 18, Academic Press, New York, 1980.
2. H. Herman, Nucl. Instr. and Meth., **182/183** (1981) 887.
3. G. Dearnaley, Rad. Eff., **63** (1982) 1.
4. M. Kopcewicz, J. Jagielski, A. Turos and D.L. Williamson, J. Appl. Phys., **71**(9) (1992) 4217.
5. K.H. Jack, Acta Cryst., **5** (1952) 404.
6. D.H. Jack, Mat. Sci. Eng. **11** (1973) 1.
7. G. Marest, Def. and Diff. Forum, **57-58** (1988) 273.
8. N. Moncoffre, M. Brunel, P. Deydier, J. Tousset, Surf. and Interf. Analysis, **9** (1986)139.
9. N. Moncoffre, Materials Science and Eng., **90** (1987) 99.
10. S. Fayeulle, G. Marest, N. Moncoffre, J. Tousset, Applied Surface Science, **32** (1988) 141.
11. G. Linker, Solid State Com.,**57**, (1986) 773.
12. D.L. Williamson, F.M. Kustas, D.F. Fobare, M.S. Misra, J.Appl. Phys, **60** (1986) 1493.
13. G. Gawlik, J. Jagielski and A. Podgórski, phys. stat. sol. (a) **95** (1986) 453.

FIGURE CAPTIONS

Fig. 1. CEMS spectra recorded for XC06 samples non implanted (a), implanted with 50 keV nitrogen ions at different fluences : 5 x 10^{16}ions.cm^{-2} (b), 10^{17}ions.cm^{-2} (c), 2 x 10^{17} ions.cm^{-2} (d), 3 x 10^{17}ions.cm^{-2}(e), 4 x 10^{17}ions.cm^{-2}(f).

Fig. 2. Relative contributions of different phases detected in the CEMS experiment.

Fig. 3. GIXD spectra recorded for the XC06 samples implanted with nitrogen ions. Incidence angle of 0.5^{o} (a) and 2.0^{o} (b).

Fig. 4. The details of the GIXD spectra showing the fits of iron peaks to the Gaussian function.

Fig. 5. Variation of strain of the underlying Fe structure as a function of dose.

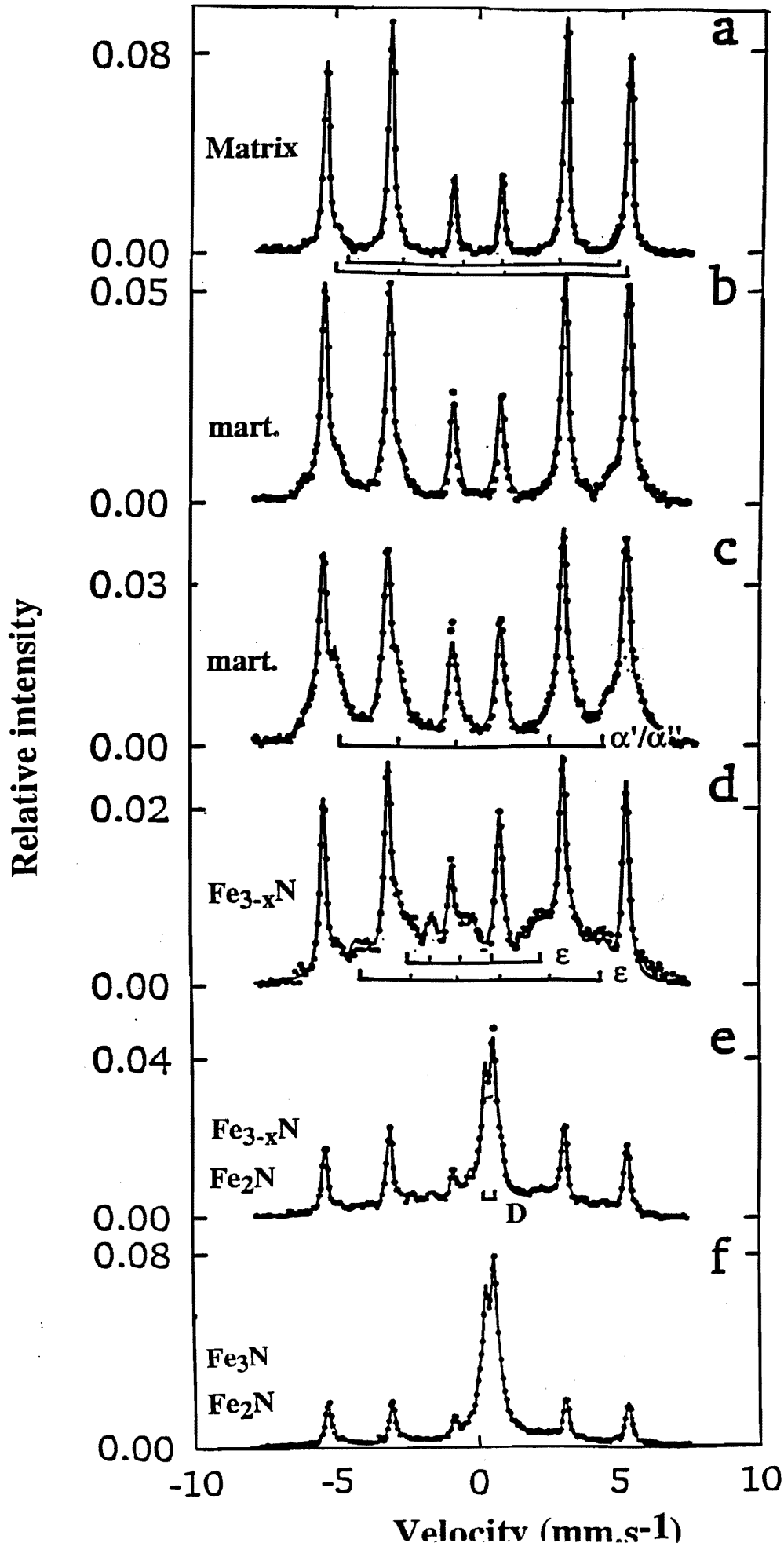
a
Matrix
0.08
0.00
b
mart.
0.05
0.00
c
mart.
α'/α''
0.03
0.00
d
Fe3-xN
ε
ε
0.02
0.00
e
Fe3-xN
Fe2N
D
0.04
0.00
f
Fe3N
Fe2N
0.08
0.00
Relative intensity
-10
-5
0
5
10
Velocity (mm.s-1)

FIG. 1

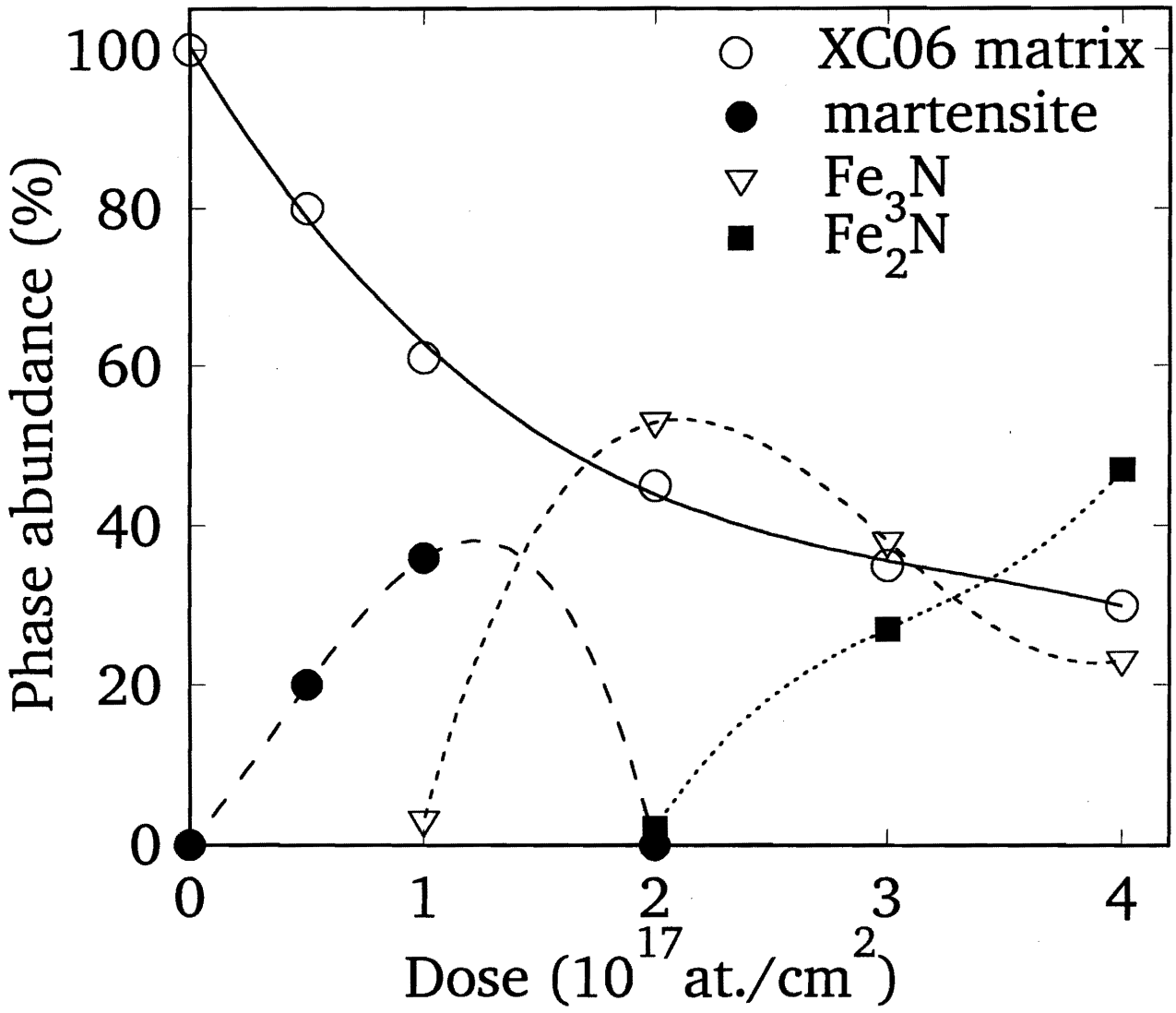
XC06 matrix
martensite
Fe_3N
Fe_2N
Phase abundance (%)
100
80
60
40
20
0
0
1
2
3
4
Dose (10^{17} at./cm^2)

FIG. 2

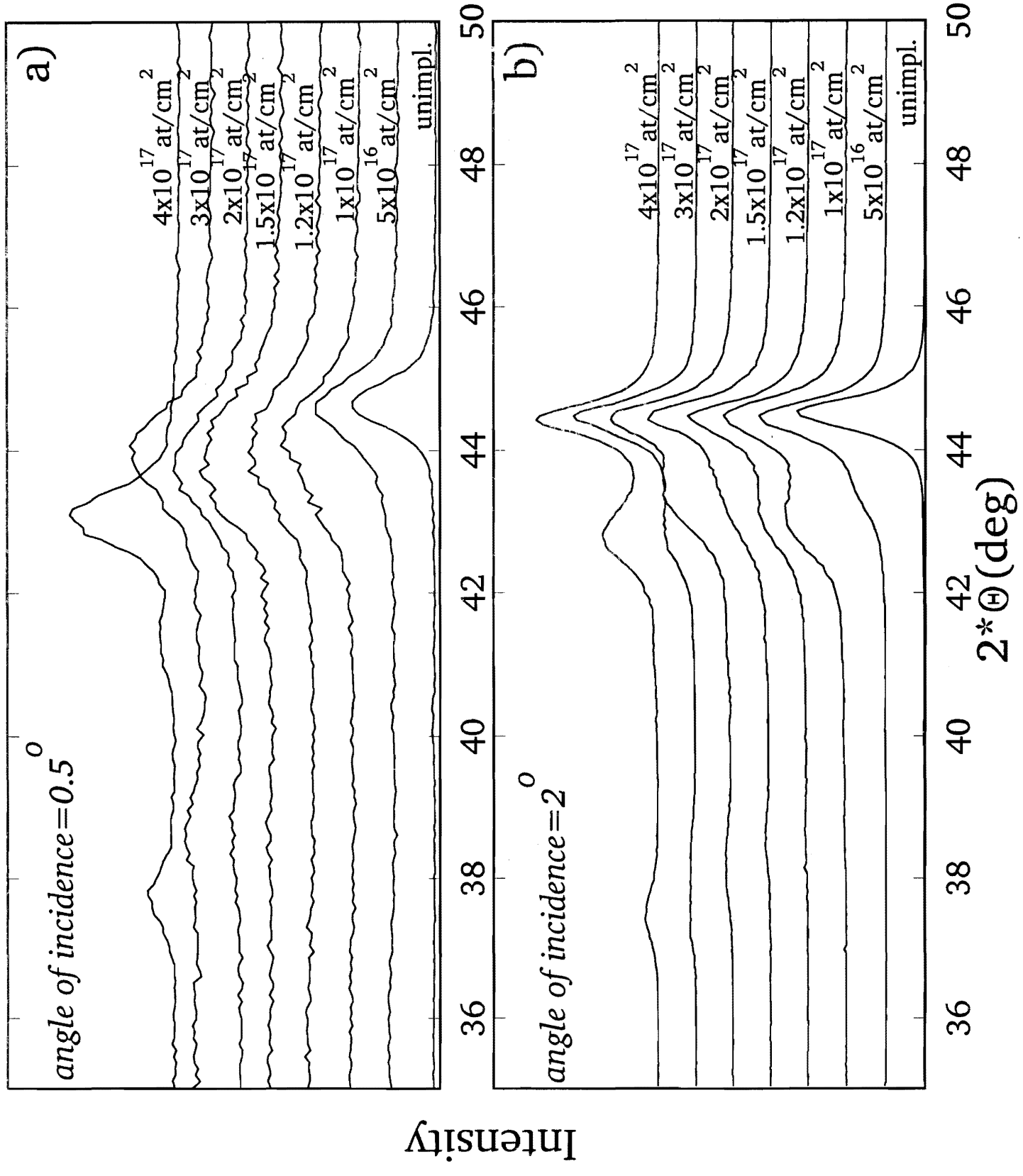
a)
angle of incidence=0.5°
4x10^17 at/cm^2
3x10^17 at/cm^2
2x10^17 at/cm^2
1.5x10^17 at/cm^2
1.2x10^17 at/cm^2
1x10^17 at/cm^2
5x10^16 at/cm^2
unimpl.
b)
angle of incidence=2°
4x10^17 at/cm^2
3x10^17 at/cm^2
2x10^17 at/cm^2
1.5x10^17 at/cm^2
1.2x10^17 at/cm^2
1x10^17 at/cm^2
5x10^16 at/cm^2
unimpl.
36
38
40
42
44
46
48
50
2*Θ(deg)
Intensity

FIG. 3

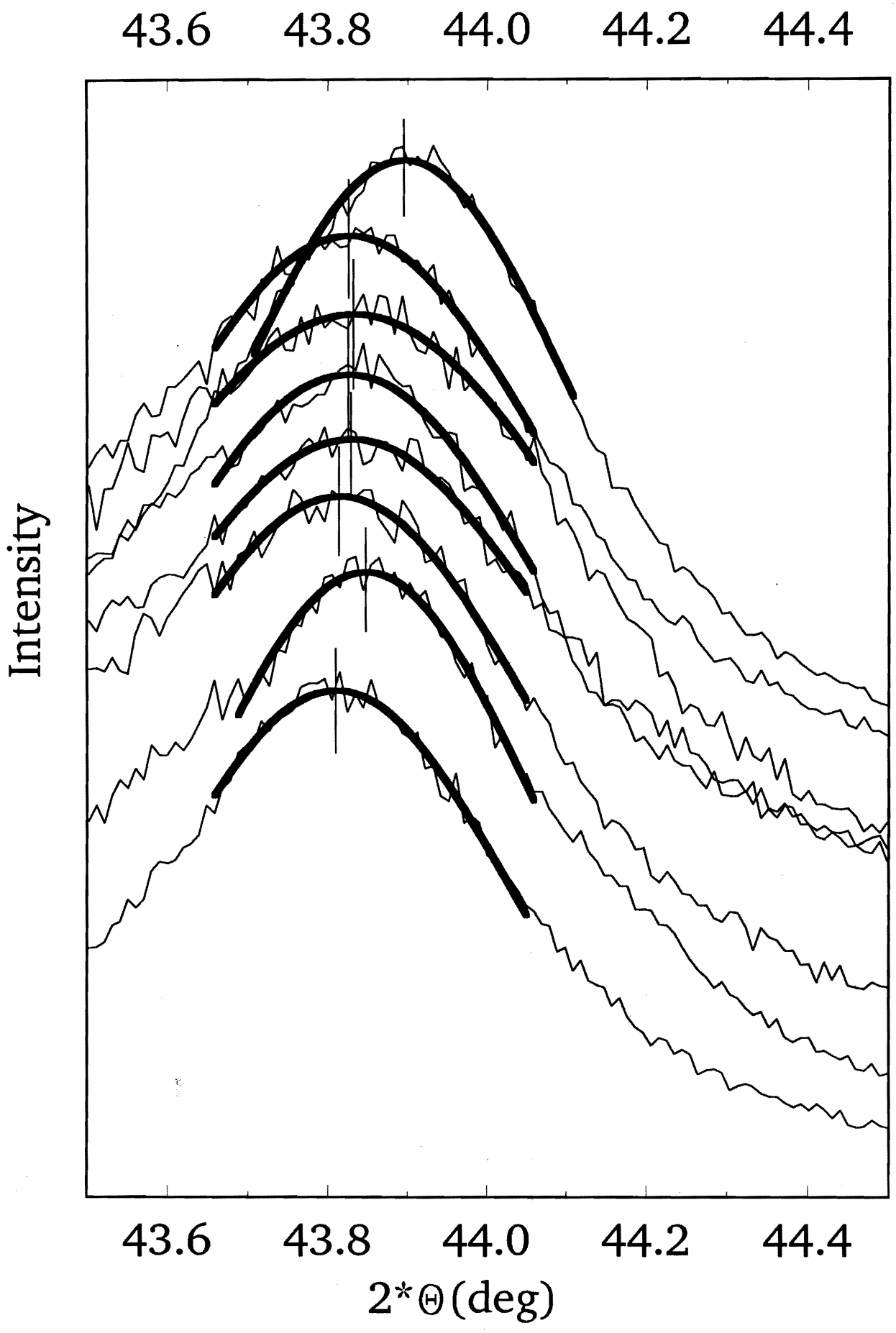

FIG. 4

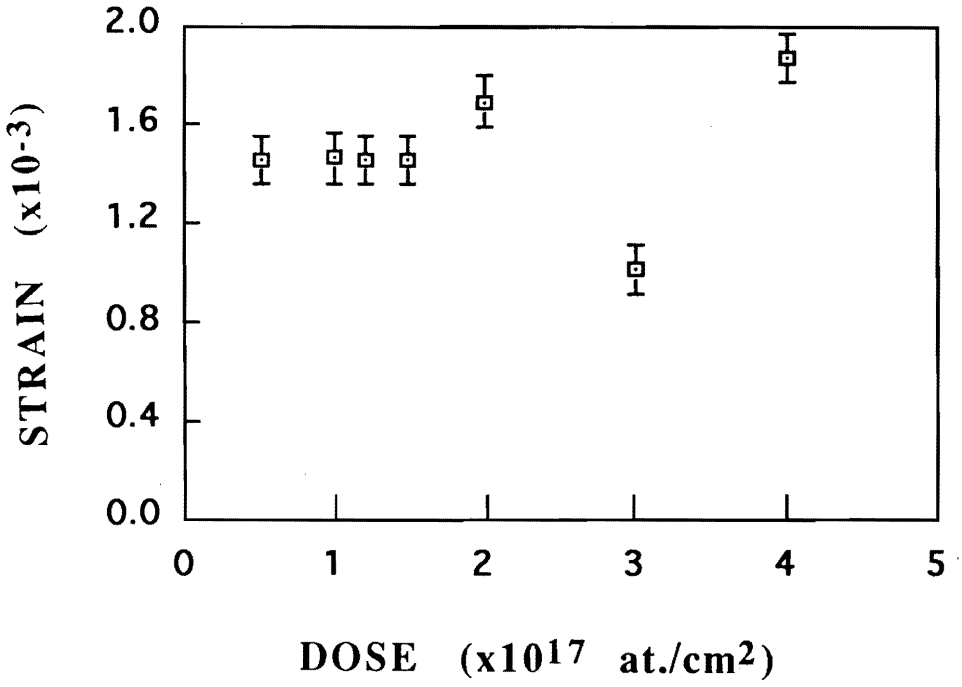
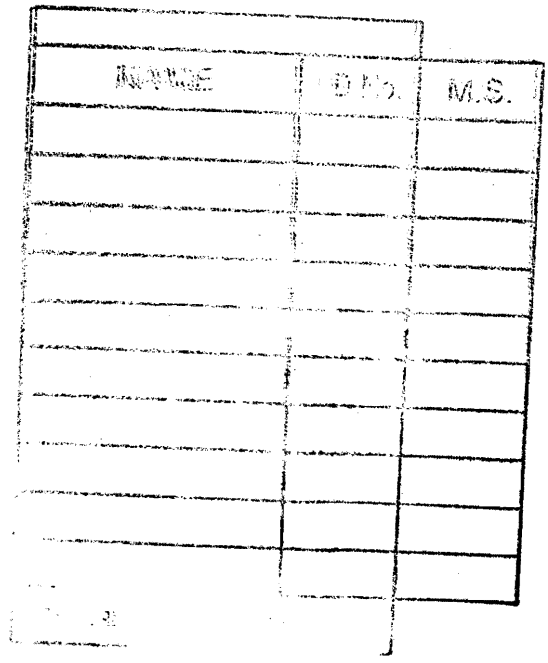
FIG. 5